Fiber Bragg Gratings for distributed cryogenic temperature measurement in a tube in tube helically coiled heat exchanger

Bharathwaj V*, Markan A†, Atrey M†, Neumann H* and Ramalingam R*

*Cryogenics Division, Institute for Technical Physics, Karlsruhe Institute for Technology, Campus North, Eggenstein –Lepoldshafen, Germany

†Department of Mechanical Engineering, Indian Institute of Technology Bombay, Mumbai, India

Email: rajini-kumar.ramalingam@kit.edu

Abstract—**A novel technique to measure the cryogenic temperature distribution of a helically coiled Tube-in-Tube (TIT) heat exchanger using Fiber Bragg Grating (FBG) array has been reported. The measured temperature distribution will help in estimating the heat exchanger efficiency and will be used to investigate its performance. The measurement of the temperature distribution has previously only been simulated, as using a standard temperature sensor would inadvertently hamper the flow. This issue can be solved by using a small sized FBG sensor array. In this paper, the principle, design and installation of sensors are explained and the initial experiments are carried out to demonstrate the measurement technique. The experimentally measured temperature distribution was found to be agreeable with the simulated values with minor deviations.**

Keywords—**Cryocoolers, Tube-in-Tube (TIT) heat exchanger, Fiber Bragg Grating (FBG), temperature measurement.**

I. Introduction

Recuperative heat exchangers are used extensively for low temperature applications, especially in Joule Thomson and Brayton cryocoolers. High effectiveness and compactness are essential characteristics for such heat exchangers. Frame and Coles [1] were among the first to suggest the use of a Tube-in-Tube (TIT) helically coiled heat exchanger for its higher heat transfer rate and compact nature. Heat exchangers have been found to play a crucial role in determining the performance of cryocoolers [2]. TIT heat exchanger can be numerically modelled in order to study its fluid flow and heat transfer characteristics. The predictive models that have been developed [3], [4] have a difficulty in defining the parameters that critically influence heat transfer characteristics. As a result, they can only give a gist of the heat transfer in a TIT heat exchanger, but not the precise temperature distribution or the heat transfer characteristics. Many researchers have also attempted to experimentally study the TIT heat exchanger [4], [5] to understand the heat transfer and fluid flow. However, the exact temperature distribution was not measured in any of these studies. Measuring the actual temperature distribution in a TIT heat exchanger can help in improving the heat exchanger design and consequently, its efficiency. Hence, in order to get the temperature profile, it is essential to measure it experimentally. The standard temperature sensor like the resistance temperature detector (e.g. PT 100) cannot be placed inside the TIT heat exchanger without obstructing the flow through it [6]. An attempt to integrate such sensors may affect the performance of the TIT heat exchanger. This brings to the fore a need for a small sized sensor that can be used to measure cryogenic temperatures. Previously Fiber Bragg Grating (FBG) sensors have been used to evaluate the temperature distribution of multilayer insulation [7]. In the present study, Bragg gratings fabricated at different locations in a single fiber is used for temperature measurement inside the TIT heat exchanger. Due to the miniature size of the FBG sensors, they can be installed inside the compact TIT heat exchanger effortlessly. Furthermore, a single fiber can have more than one sensor deployed on it, which can be achieved using wavelength division multiplexing (WDM) scheme. Accordingly, the single fiber FBG sensors do not have an impact on the flow or the performance of the heat exchanger. Hence, the exact temperature distribution achieved using FBG sensors can be used by researchers working on cryocoolers to optimize the performance of the heat exchanger.

II. Operating Principle of FBG

The light travelling through an FBG undergoes Fresnel reflection due to the periodic variation of the refractive index along the fiber core. When the broad-band light signal is transmitted along the FBG, the light is reflected back at a particular wavelength which is referred to as the Bragg wavelength (λ_B). The Bragg wavelength [8] for a FBG is given as

$$\lambda_B = 2 \cdot n_{eff} \cdot \Lambda \qquad (1)$$

where n_{eff} is the effective refractive index of the fiber core and Λ is the grating period. A single fiber has gratings with different periods that have been fabricated at a number of positions. Such an FBG sensor array attained using WDM scheme can be seen in Fig. 1. Inside the TIT heat exchanger, any slight perturbation will vary the reflected wavelength for each sensor. The changes in the reflected wavelength are recorded using the signal detection scheme shown in Fig. 2. These deviations in the Bragg wavelength occur not only due to the changes in temperature ΔT but also the induced strain, ε.

The relative shift in the Bragg wavelength is approximately given as

$$\Delta\lambda_B/\lambda_B = (\alpha_s + \alpha_n) \cdot \Delta T + (1 - p_e) \cdot \varepsilon \quad (2)$$

where p_e is the photo elastic constant, α_s is the thermal expansion coefficient and α_n is the thermal optic coefficient of the optical fiber.

III. Design and Fabrication of Heat Exchanger with FBG Sensors

To conduct the experiment, a TIT helically coiled heat exchanger is designed and fabricated with Copper chosen as the material owing to its high thermal conductivity and corrosion resistance. A baffle is utilized while winding the inner tube to provide reinforcement. It also separates the inner and the outer tubes so that they do not come in contact while coiling. The outer and the inner tubes with baffle wire are fabricated using the parameters given in Table I.

A total of 12 FBG sensors (FBG1 – FBG12) are fabricated on a single mode fiber. They are integrated with the tubes before forming the helical coil. The Bragg wavelength of these sensors are different which enables their simultaneous measurement using WDM scheme. The sensing array is installed along the inner tube and the baffles in the outer wall of the inner tube. The sensors are located at an interval of 0.6 m with six of them along the inner tube (FBG1 – FBG6) and six in the annular region (FBG7 – FBG12).

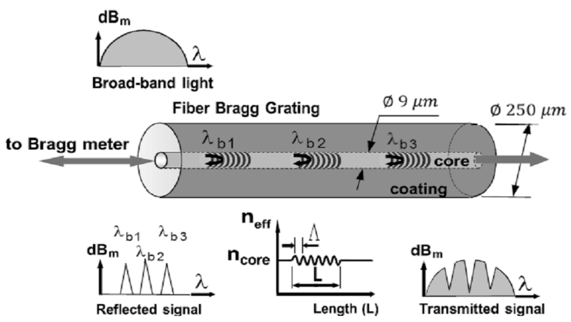

Fig. 1. General measurement scheme of FBG

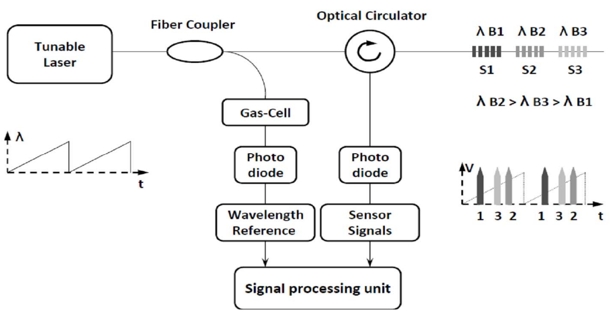

Fig. 2. Signal detection scheme

TABLE I. Heat Exchanger Parameters

Parameter	Inner Tube	Outer Tube
Tube Diameter (Minor)	5 mm	10 mm
Tube Length	3006 mm	3000 mm
Wall Thickness	0.8 mm	0.8 mm
Length of Baffle wire	3006 mm	
Pitch of Baffle wire	500 mm	

IV. Calibration of FBG Sensors

Before the start of the experimentation, the FBG sensors are calibrated between 77 K and 300 K using liquid Nitrogen. A calibrated TVO sensor is used as a reference to calibrate the FBG sensors. The change in temperature of the TVO sensor is recorded along with the change in the Bragg wavelength of the FBG sensors. This is used to calculate the sensitivity for each sensor at different temperature ranges as shown in Table II.

In order to obtain an accurate measurement of the temperature in the heat exchanger, the effects of pressure and mass flow rate are also considered. Before the setup is integrated, the cross sensitivity in the measurement of the temperature at different pressures and mass flow rates is calculated. This is done by passing Nitrogen gas at room temperature through the system at pressures ranging from 0 to 1.5 bar and at mass flow rates upto 0.8 g/s. The relative shifts in the Bragg wavelength were found to be negligible due to the changes in pressure and mass flow rate. Moreover, to ensure that the change in the Bragg wavelength is only due to the temperature, the FBG sensors were integrated in a way that the effect of strain was nullified.

V. Modelling of TIT Heat Exchanger

The TIT helically coiled heat exchanger was modelled prior to the experiments. The objective was to determine the temperature distribution in a counter-flow TIT heat exchanger and to study the behaviour of fluid flow and heat transfer. COMSOL Multiphysics is utilized to carry out the simulation where the hot fluid enters through the inner tube and the cold fluids flows out through the annular region. A three-dimensional axisymmetric model with baffles is employed. ‘Highly conductive layer’ boundary condition is used to model

TABLE II. Sensitivity of Sensors

Sensors	Sensitivity (pm/K)				
	Temperature Range (K)				
	77-100	*100-150*	*150-200*	*200-250*	*250-300*
FBG1	6.25	8.85	10.35	13	12
FBG2	9.06	8.85	10.1	12.5	11.5
FBG3	10	8.25	10.9	13	12
FBG4	11.125	8.5	10.5	11.5	12
FBG5	9.375	8.5	10.5	13	11.5
FBG6	9.375	8.5	11.5	13	11.5
FBG7	10	8.5	11	13.5	11.5
FBG8	9.375	8.5	11.5	13.5	11.5
FBG9	8.125	9.5	11.5	12.5	10.5
FBG10	10	8.85	10.85	13	11.5
FBG11	9.375	8.5	10.85	13.85	11.5
FBG12	10	8.5	10.85	13.85	11.5

the thickness of the inner tube. This feature is efficient for modelling heat transfer in thin layers made of a good thermal conductor. The model parameters are the same as those previously shown in Table I. For the model, the material used is gaseous Nitrogen whereas Copper is taken as the material for the highly conductive layer. The k-ε turbulent flow model of Patankar et al. [9] is used to simulate the flow. The boundary conditions that are applied to the model are shown in Table III. The simulation assumes steady and incompressible flow. Also, radiation effects are considered to be negligible and properties of materials are calculated at the mean temperature. Taking into consideration the mentioned assumptions and boundary conditions, the simulation is carried out for an inlet velocity of 12 m/s. The temperature distribution along the TIT heat exchanger obtained from the simulation is later used to compare with the experimental results.

VI. Experimental Study

A. Experimental Setup

An outline of the experimental setup is shown in Fig. 3. The TIT heat exchanger fitted with the FBG sensors is enclosed by a cryostat which functions as a vacuum chamber necessary for the experiment. The cryostat also carries an inner block which is used to store liquid Nitrogen for cooling the working fluid. The level of liquid Nitrogen in the inner block is determined by using two PT 100 temperature sensors with one each connected at the inlet and the outlet of the inner block, respectively. The sensing fiber array is taken out from the cryostat using a feed-through which ensures that there is no loss in vacuum. The fiber is then connected to the Bragg meter to measure the Bragg wavelength.

B. Experimental Procedure

The arrangement as shown in Fig. 3 is laid out. The mass flow meter and manometer are connected to the system. Once the system is assembled, it was subjected to a leak test to account for vacuum inside the cryostat and to ensure that the system is without any leaks. A vacuum of about 10^{-3} to 10^{-4} mbar is required to conduct the experiment. The vacuum pump is used to maintain vacuum inside the cryostat throughout the experiment. The working fluid is warm Nitrogen gas which is first passed through the system in order to flush out the air present in the heat exchanger. Liquid Nitrogen is then filled inside the inner block and the two PT 100 sensors are used to determine when the inner block is completely filled.

TABLE III. Boundary Conditions for Simulation

Boundary	Fluid	Heat Transfer
Inner Tube		
Inlet	Velocity = 12 m/s	Temperature = 293 K
Outlet	Outflow	Outflow
Walls	Wall	Highly Conductive Layer
Outer Tube (Annulus)		
Inlet	Velocity = 12 m/s	Temperature = 78 K
Outlet	Outflow	Outflow
Walls	Wall	Highly Conductive Layer or Thermal Insulation

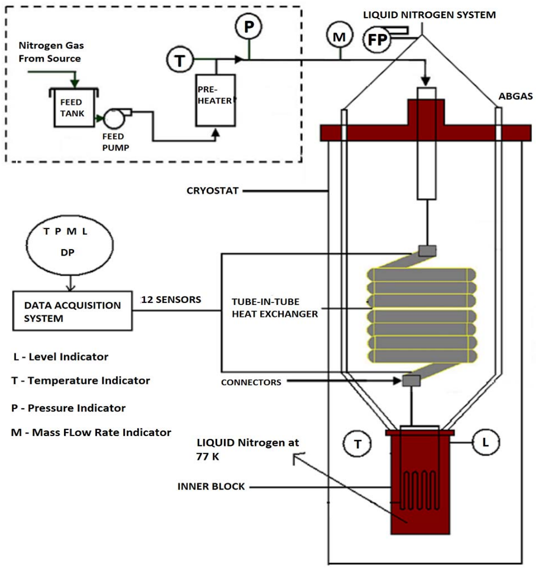

Fig. 3. Experimental setup

Once liquid Nitrogen is filled, the warm Nitrogen gas is passed through the inlet of the heat exchanger and it flows through the inner tube into the inner block containing liquid Nitrogen and comes out through the annulus region, i.e. counter flow takes place in the heat exchanger. Two different sets of experiments are conducted. In the first test (Test 1), the pressure of the working fluid is increased in steps of 0.5 bar from 0 to 1.5 bar and then finally brought down back to zero. In the second test (Test 2), the pressure is directly increased to 1.6 bar and is maintained for the steady state to be achieved. During these tests, the changes in wavelengths are recorded using the Bragg meter for all the sensors so as to get an idea of the temperature distribution inside the TIT helically coiled heat exchanger. However, during the experimentation, the feed-through for the fiber of the latter four sensors (FBG9 – FBG12) did not function properly and it was not possible to measure the wavelength shifts from these sensors.

VII. Results and Discussions

Using the wavelength shifts measured by the Bragg meter and the sensitivity values from Table II, the corresponding changes in the temperature are attained for both the tests. Fig. 4 shows the change in the temperature with time for the eight sensors during Test 1. As can be seen, the sensors FBG6 and FBG7 are already stable near the liquid Nitrogen temperature since they are in the vicinity of the inner block. The temperature at other sensors falls slowly as the mass flow rate of the working fluid is small. At about 200 seconds after the start, the pressure is increased from 0.5 bar to 1 bar causing the mass flow rate to increase which leads to a steep decline in the temperature. After approximately 650 seconds, the pressure is further increased to 1.5 bar which can be seen by a further dip in the temperatures for the first five sensors. However, at the end of the test, the first four sensors are not able to attain steady state temperatures.

The temperature deviation with time during Test 2 can be seen in Fig. 5. The temperatures of sensors FBG6 and FBG7 fall almost instantly to a temperature close to 77 K. Unlike Test 1, steady state temperatures are achieved by all sensors in Test 2. Fig. 6 displays the temperature distribution along the inner tube for the two tests and the simulation. The tests show slight deviation from the simulation results probably due to simulations assuming ideal conditions and FBG sensor calibration not being perfect. Also, it can be seen that the temperatures along the inner tube in Test 2 were lower than those in Test 1 particularly in the case of sensor FBG2. This can be due to the fact that steady state had not been achieved for all the sensors in Test 1.

A. *Heat Transfer Characteristics*

Since the exact temperature distribution along the TIT heat exchanger is determined, the actual heat transfer characteristics can be calculated. However, due to incomplete temperature data for the outer tube, the values from simulation are used for the failed sensors. Table IV shows some of the heat transfer characteristics for both the tests and the simulation.

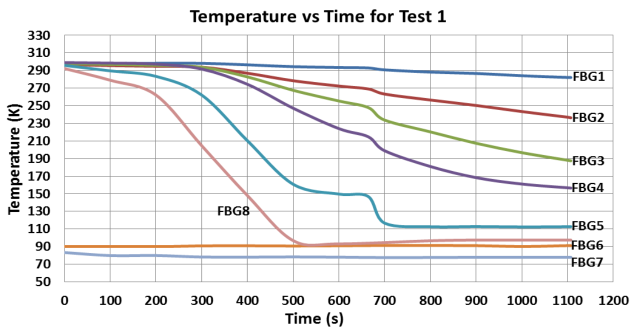

Fig. 4. Transient temperature for sensors FBG1−FBG8 for Test 1

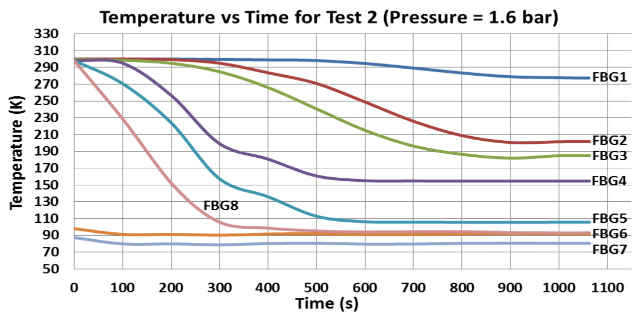

Fig. 5. Temperature variation with time of sensors for Test 2

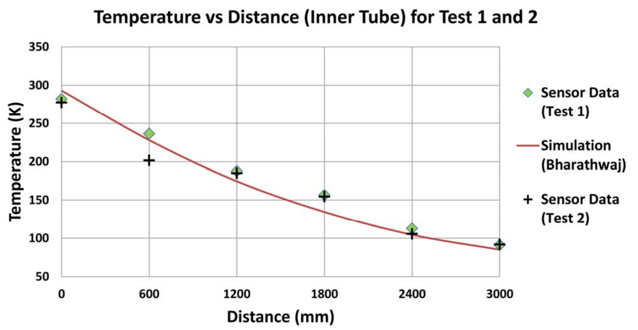

Fig. 6. Temperature distribution along the inner tube of the heat exchanger

TABLE IV. HEAT TRANSFER CHARACTERISTICS

Parameters	Test 1	Test 2	Model
Velocity (m/s)	7.03	10.61	12
Mass Flow Rate (g/s)	0.431	0.677	0.736
Inner Tube Inlet Temperature (K)	282.12	277.41	293
Inner Tube Outlet Temperature (K)	91.13	91.85	85
Outer Tube Inlet Temperature (K)	77.91	80.54	78
Heat Transfer Rate (W)	86.699	132.451	161.448
Maximum Heat Transfer Rate (W)	94.296	141.695	169.642
Heat Exchanger Effectiveness	0.919	0.935	0.952

It can be seen that the heat transfer rate for Test 1 is lower as compared to Test 2 due to lower mass flow rate. Also, the heat exchanger effectiveness of the first test is slightly lesser than that for the second test. This is probably due to the fact that steady state had not been attained in Test 1 and hence, complete heat transfer may not take place.

VIII. CONCLUSION

FBG sensors have been successfully used for temperature measurement in a TIT helically coiled heat exchanger. Two sets of experiments were carried out and the measured temperature distribution was compared with the simulated values. It was found that the measured values deviate approximately 15 % from the simulated value. This could be due to the fact that the simulation assumes the heat exchange to be perfect whereas there may be certain inefficiencies in the system. The heat transfer characteristics of the heat exchanger are analyzed to further scrutinize the performance of the heat exchanger. From the results obtained, it can be inferred that the use of FBG sensors could provide researchers with a unique method for temperature measurement in a TIT heat exchanger.

REFERENCES

[1] Coles, D.K. and Frame, W.R., “Joule-Thomson effect gas liquefier,” U.S. Patent 3 048 021, August 7, 1962.

[2] N.S. Walimbe, K.G. Narayankhedkar, M.D. Atrey, “Experimental investigation on mixed refrigerant Joule–Thomson cryocooler with flammable and non-flammable refrigerant mixtures,” Cryogenics, vol. 50, no. 10, pp. 653–659, 2010.

[3] T.J. Rennie, V.G.S. Raghavan, “Numerical studies of a double-pipe helical heat exchanger,” Appl. Therm. Eng., vol. 26, pp. 1266–1273, 2006.

[4] V. Kumar, S. Saini, M. Sharma, K.D.P. Nigam, “Pressure drop and heat transfer study in tube-in-tube helical heat exchanger,” Chem. Eng. Sci., vol. 61, pp. 4403–4416, 2006.

[5] T.J. Rennie, V.G.S. Raghavan, “Experimental studies of a double-pipe helical heat exchanger,” Exp. Therm. Fluid Sci., vol. 29, pp. 919–924, 2005.

[6] P.M. Ardhapurkar, A. Sridharan, M.D. Atrey, “Performance evaluation of heat exchanger for mixed refrigerant J–T cryocooler,” Cryogenics, 2014, in press.

[7] R. Ramalingam, H. Neumann, “Fiber Bragg Grating-based temperature distribution evaluation of multilayer insulations between 300 K–77 K,” IEEE Sensors J., vol. 11, no. 4, 2011.

[8] A. Othonos and K. Kalli, Fiber Bragg Gratings – Fundamentals and Application in Telecommunications and Sensing. Norwood, MA: Artech House, 1999.

[9] Patankar, S.V., Pratap, V.S., Spalding, D.B., “Prediction of turbulent flow in curved pipes,” Journal of Fluid Mechanics, vol. 67, pp. 583–595, 1975.